

# Study on Boron–Hydrogen Pairs in Bare and Passivated Float-Zone Silicon Wafers


Clemens Winter, Jochen Simon,\* and Axel Herguth

This study deals with the dynamics of the formation and dissociation of boron–hydrogen (BH) pairs in crystalline silicon during a rapid high-temperature treatment and subsequent dark annealing between 200 and 300 °C. Highly accurate resistivity measurements are used to detect BH pairs in chemically polished B-doped float-zone silicon. It is found that an unexpected high amount of hydrogen is present in the as-purchased wafers. Hydrogen is initially mostly paired to boron but can be dissolved by a short high-temperature firing step. If a firing step (530 °C) is applied to bare, unpassivated Si wafers, most of the initial BH pairs are dissolved, and hydrogen dimers (H<sub>2</sub>) form. With increasing peak temperature, an increasing amount of hydrogen leaves the H<sub>2</sub> ⇌ BH system, while the proportion of BH increases. Additional hydrogen can be introduced by firing a wafer passivated with plasma-enhanced chemical vapor deposition (PECVD) SiN<sub>x</sub>:H. A three-state model shows a good agreement with the measured data for both bare and coated samples as well as for different annealing temperatures. With increasing dark annealing temperatures, the BH dynamics accelerates, whereas the maximum BH concentration reached decreases. For temperatures above 280 °C, significant changes in the reaction dynamics are observed.

## 1. Introduction

The role of hydrogen in crystalline silicon (c-Si) has been studied for decades due to its multifaceted properties. Hydrogen is known to passivate defects both in the bulk and at the surface<sup>[1–4]</sup> and can deactivate dopant atoms, both in p- and n-type c-Si due to its amphoteric nature.<sup>[4,5]</sup> It also plays an important role in different degradation phenomena. For the permanent deactivation of the boron–oxygen complex, which is responsible for light-induced degradation of charge carrier lifetime, hydrogen is needed.<sup>[6]</sup> In recent years, the presumed importance of hydrogen in light and elevated temperature-induced degradation (LeTID)<sup>[7–10]</sup> has drawn even

C. Winter, J. Simon, A. Herguth  
Department of Physics  
University of Konstanz  
78457 Konstanz, Germany  
E-mail: jochen.simon@uni-konstanz.de

 The ORCID identification number(s) for the author(s) of this article can be found under <https://doi.org/10.1002/pssa.202100220>.

© 2021 The Authors. physica status solidi (a) applications and materials science published by Wiley-VCH GmbH. This is an open access article under the terms of the Creative Commons Attribution-NonCommercial License, which permits use, distribution and reproduction in any medium, provided the original work is properly cited and is not used for commercial purposes.

DOI: 10.1002/pssa.202100220

more attention from the photovoltaics community to improve the understanding of the various hydrogen interactions in silicon.

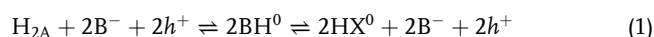
Unfortunately, the direct quantification of hydrogen with methods such as secondary ion mass spectrometry (SIMS) or low-temperature Fourier-transformed IR spectroscopy achieves only relatively high detection limits. The tendency of hydrogen to bind to dopant atoms as the most available impurity opens up an alternative, indirect way of hydrogen quantification. The formation of boron–hydrogen (BH) pairs from H<sub>2</sub> in boron-doped silicon consumes a hole and, thereby, negates the doping effect of boron.<sup>[11]</sup> In the past, this effect on the sample's resistivity has been widely used to study BH dynamics.<sup>[1,2,12,13]</sup> In this contribution, highly sensitive resistance measurements<sup>[14]</sup> are used to investigate BH dynamics, which achieve a detection limit significantly lower than those based on contactless eddy-current measurements

recently presented in the study given by Walter et al.<sup>[13]</sup>

Hydrogen often originates from hydrogen-rich dielectric films such as silicon nitride (SiN<sub>x</sub>:H), which release hydrogen during high-temperature steps. Within this contribution, the impact of rapid high-temperature steps on BH pair dynamics in bare and SiN<sub>x</sub>:H-passivated float-zone silicon (FZ-Si) samples during dark annealing at 220 °C is investigated. Furthermore, the influence of the dark annealing temperature in the range 200–300 °C is studied.

## 2. BH Pairs and Electrical Resistance

In impurity-lean silicon such as FZ-Si, hydrogen is predominantly present in the form of dimers (H<sub>2</sub>) or attached to dopants, in our case boron, due to its high reactivity.<sup>[15]</sup> As discussed later on, hydrogen may change between those states according to the left-hand side of the reaction scheme



where the dissociation of the (H<sub>2A</sub>)<sup>[16]</sup> dimer consumes two holes. It should be noted that the left-hand side of the reaction scheme is different from the description used in the model of Voronkov and Falster,<sup>[16]</sup> because only the net effects on charge carrier concentration are considered. It is, furthermore, observed that BH pairs may vanish as well under the very same conditions known to trigger the formation, hence suggesting that hydrogen changes its binding state in the long run for a second time

(right-hand side of the above-mentioned reaction scheme). During this subsequent reaction, holes are released again, which implies that hydrogen occupies an electrically neutral, more favorable binding state  $HX^0$ . It cannot be excluded that hydrogen binds to itself ( $X = H$ ), however, in a different dimeric configuration ( $H_{2c}$ ) as suggested by Voronkov and Falster.<sup>[16]</sup> An alternative explanation could be the effusion as neutral species. Assuming first-order reaction kinetics, the concentration of BH pairs is described by a sum of two exponential functions

$$[BH](t) = -A_1 \cdot \exp(-t/t_1) + A_2 \cdot \exp(-t/t_2) + A_\infty \quad (2)$$

with time constants  $t_{1,2}$  and amplitudes  $A_{1,2}$ , where the index 1 represents the formation, and index 2 the dissociation of BH pairs, whereas  $A_\infty$  giving the long-term limit. The introduction of the second exponential function extends the model from the study given by Voronkov and Falster<sup>[16]</sup> and allows for a description of the measured data, as will be explained later on. The electrical resistivity  $\rho$

$$\rho^{-1} = q \times (p \times \mu_p + n \times \mu_n) \quad (3)$$

is given by the elementary charge  $q$ , hole and electron concentration  $p, n$ , and their associated mobility  $\mu_{p,n}$ . For p-type material without any excess charge carriers,  $n$  is negligible, and  $p$  is equivalent to the equilibrium hole concentration  $p_0$ , which, in turn, is mainly determined by the (ionized) doping concentration  $N_{dop}$ . Considering Equation (1), where deactivation of boron is caused by the formation of BH pairs, it follows

$$\rho^{-1} = q \times \mu_p \times (N_{dop} - [BH]) \quad (4)$$

This gives a direct measure for the concentration of BH pairs via resistance measurements.

### 3. Experimental Section

As purchased, chemically polished FZ-Si wafers, B-doped with  $N_{dop} \approx 1.5 \times 10^{16} \text{ cm}^{-3}$  ( $\rho \approx 1 \Omega \text{ cm}$ ) and a thickness of  $250 \mu\text{m}$ , are cut into  $5 \times 5 \text{ cm}^2$  samples. On some samples, hydrogen-rich silicon nitride ( $\text{SiN}_x\text{:H}$ ) is deposited on both sides via plasma-enhanced chemical vapor deposition (PECVD) in a PlasmaLab100 reactor from Oxford Instruments (deposition temperature  $400^\circ\text{C}$ , total duration 12 min per side). By adjusting the ratio of the gas flows of ammonia ( $\text{NH}_3$ ) and silane ( $\text{SiH}_4$ ), 100 nm thick  $\text{SiN}_x\text{:H}$  layers of different composition are produced observable by a variation in refractive indices  $n$  being 2.10, 2.40, and 2.55 at 630 nm, respectively. The samples were not subjected to any wet chemical treatment beforehand, meaning that the thin layer of silicon oxide wet-chemically grown by the wafer manufacturer is still present on all samples. Most of the samples receive a short high-temperature step in a conveyor belt furnace (“firing step”), with sample peak temperatures ( $T_F$ ) between  $500$  and  $850^\circ\text{C}$ . The samples’ temperature is monitored with a K-type thermocouple mechanically pressed onto the wafer surface. The set peak temperature of the belt furnace is adjusted in a way that the actual sample peak temperature  $T_F$  matches the targeted temperature as closely as possible. Such a firing process, which is commonly used for metal contact formation on Si solar cells, is also known to release

hydrogen from the  $\text{SiN}_x\text{:H}$  layer into the Si bulk.<sup>[17]</sup> The steep cool-down ramp leaves most of the hydrogen in the Si bulk in an electrically inactive state,<sup>[15,18]</sup> which can be identified by the dimeric configuration  $H_{2A}$ .<sup>[16]</sup> During a subsequent dark annealing on a hotplate (Prazitherm) at a temperature  $T_{DA}$ , the reaction described in Equation (1) is triggered, which is accompanied by a change in resistivity as described earlier.

To quantify these changes, highly accurate four-terminal electrical resistance measurements are performed. More details and a thorough error analysis of the methodology are published elsewhere.<sup>[14]</sup> Electrical contacts to the silicon are established with two parallel double stripes of thermally evaporated aluminum (Al) (see **Figure 1**). Highly Al-doped  $p^+$  regions are created by a pattern of laser pulses (laser-fired contacts [LFCs]),<sup>[19]</sup> enabling a reliable and low resistance contact. Neither Al evaporation nor the creation of LFCs cause significant temperature load on the sample. A digital multimeter (Keithley 2000, 6.5 digit) is used for the resistance measurements. As temperature control is a crucial factor for highly accurate measurements,<sup>[14]</sup> they are performed on a temperature stabilized stage ( $T = 25.0^\circ\text{C}$ ) inside a light-tight housing. The dark annealing treatment is briefly interrupted for each measurement point.

With respect to the chosen cuboid sample geometry and under the assumption of a homogeneous resistivity  $\rho$  in the total volume tested, resistance  $R$  is given by

$$R = \rho \times \frac{g \times d}{w \times t} \quad (5)$$

with distance of the inner electrodes  $d = 40 \text{ mm}$ , sample thickness  $t = 250 \mu\text{m}$ , and width  $w = 50 \text{ mm}$ . A geometry factor  $g = 1.02$  is used for compensation of a slightly inhomogeneous current distribution. It should be noted that due to the integral nature of the resistance measurement, it is impossible to draw conclusions on the (in)homogeneity of resistivity, in particular, in terms of depth. However, as most (but not all) of the samples used are subjected to a firing step during which homogenization of hydrogen in depth is expected, the assumption of a constant resistivity seems justified. Combining this equation with Equation (4) and taking the difference between two measurements, the following expression is obtained for the difference in BH pairs  $\Delta[BH]$  with respect to a reference point

$$\Delta[BH] = \frac{g \times d}{q \times w \times t} \times \left( \frac{1}{\mu_{p,0} \times R_0} - \frac{1}{\mu_p \times R} \right) \quad (6)$$

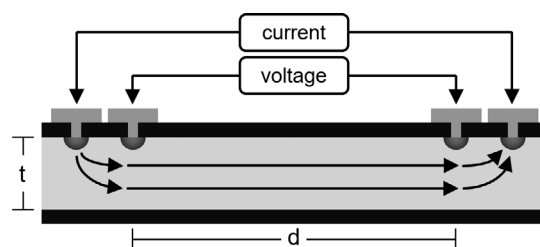


**Figure 1.** Cross section of the sample structure, not to scale. The aluminum contacts (gray) are fired through the  $\text{SiN}_x\text{:H}$  layer (black, only present on some samples) and form a highly doped  $p^+$  region underneath (dark gray) inside the Si bulk (light gray).

Taking the difference ensures that  $N_{\text{dop}}$  no longer appears as a parameter and does not have to be known exactly. Mobilities are calculated with an online tool from PV lighthouse<sup>[20]</sup> using the approach described in the study given by Herguth and Winter.<sup>[14]</sup> The choice of the reference resistance value  $R_0$  is arbitrary and is given in the following in each case. It should be noted that this measurement method interprets all changes in resistance as a change in  $\Delta[\text{BH}]$ .

#### 4. Experimental Results and Discussion

The first part of this section covers the evolution of BH pair concentration during a dark anneal at 220 °C of FZ-Si samples, which have a hydrogen-rich  $\text{SiN}_x\text{:H}$  layer on both sides. The samples were subjected to a short high-temperature firing step before annealing to introduce hydrogen from the  $\text{SiN}_x\text{:H}$  into the Si bulk. In the second part, the effect of a dark anneal on bare FZ-Si with no obvious hydrogen source is investigated. In the last part, the dark annealing temperature is varied between 200 and 290 °C to determine the critical temperature at which BH pairs do not form any longer.

##### 4.1. Evolution of BH Pairs in FZ-Si with a $\text{SiN}_x\text{:H}$ Layer

For each refractive index ( $n = 2.10, 2.40, \text{ and } 2.55$ ), three samples were prepared and subjected to a high-temperature firing step at the peak temperatures of  $\approx 735, 790, \text{ and } 850$  °C, respectively. In **Figure 2a**, the dynamics of the BH pairs during a subsequent dark anneal at  $T_{\text{DA}} = 220$  °C is displayed. The firing temperature is represented by the color, whereas the symbols indicate the refractive index of the  $\text{SiN}_x\text{:H}$ . The long-term limit was used as the reference point for calculating  $\Delta[\text{BH}]$ , so all

curves approach zero for long times. The overall behavior of the samples is quite comparable: A concentration of  $0.7\text{--}2 \times 10^{14} \text{ cm}^{-3}$  BH pairs is already present after firing. During dark annealing, BH pairs form from  $\text{H}_{2\text{A}}$  according to Equation (1), resulting in a rise of  $\Delta[\text{BH}]$ . The maximum concentration reached after a couple of hours at 220 °C varies from less than  $1.7 \times 10^{14} \text{ cm}^{-3}$  to almost  $11 \times 10^{14} \text{ cm}^{-3}$  where higher concentrations are reached with higher firing temperatures. The different compositions of the  $\text{SiN}_x\text{:H}$  layers (characterized by different refractive indices) seem to play a minor role only, which is in contrast to previous reports.<sup>[21]</sup> However, one should note that different PECVD tools (here: direct plasma, and the study by Bredemeier et al.<sup>[21]</sup> remote plasma) were used, and layers might differ more in their microscopic structure than what is revealed in the refractive index. The maximum concentration of BH pairs  $\Delta[\text{BH}]_{\text{max}}$  is composed of the initial concentration  $\Delta[\text{BH}]_{t=0\text{h}}$  and the share  $\Delta[\text{BH}]_{\text{DA}}$ , which indicates how many additional BH pairs form during dark annealing

$$\Delta[\text{BH}]_{\text{max}} = \Delta[\text{BH}]_{t=0\text{h}} + \Delta[\text{BH}]_{\text{DA}} \quad (7)$$

The initial concentration  $\Delta[\text{BH}]_{t=0\text{h}}$  contains information about the post-firing state and is independent of the dark anneal.  $\Delta[\text{BH}]_{\text{DA}}$ , on the other hand, depends on both the initial concentration of  $\text{H}_{2\text{A}}$  and the dark anneal during which the reaction  $\text{H}_{2\text{A}} \rightarrow \text{BH}$  takes place. To separate these influences, the respective dependence of the two quantities on the firing temperature will be considered individually. In the upper graph of Figure 2b, it is shown that  $\Delta[\text{BH}]_{t=0\text{h}}$  (brown) doubles from 730 to 850 °C, whereas  $\Delta[\text{BH}]_{\text{DA}}$  (blue) increases almost tenfold from  $1 \times 10^{14}$  to  $9 \times 10^{14} \text{ cm}^{-3}$ . Thus, at higher firing temperatures, significantly more hydrogen is introduced into the Si volume, which is in accordance with a previous study.<sup>[6]</sup> Directly after firing, most

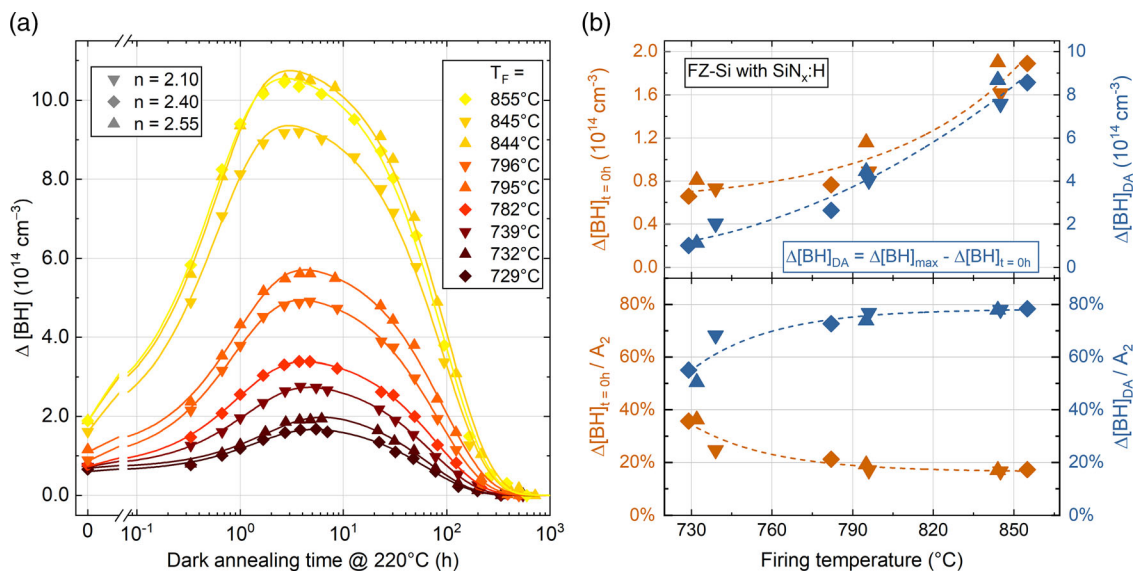


**Figure 2.** a) Change in BH pair concentration of FZ-Si samples with different refractive indices and firing temperatures during a dark anneal at  $T_{\text{DA}} = 220$  °C. The long-term limit is used as the reference point for calculation of  $\Delta[\text{BH}]$ . The lines are double exponential fits to the measurements according to Equation (2). b) Initial concentration  $\Delta[\text{BH}]_{t=0\text{h}}$  (brown) and increase of BH pairs during dark annealing  $\Delta[\text{BH}]_{\text{DA}}$  (blue) as a function of firing temperature. The upper graph shows absolute values, whereas the lower displays the ratio of the two quantities to the fit parameter  $A_2$ . The lines are empirical trend lines.

of the hydrogen is present in the form of  $H_{2A}$ . The increase in  $\Delta[BH]_{t=0h}$  with higher peak temperatures shows that the absolute amount of BH pairs already present after firing rises as well. Under the assumption that at the beginning of the dark anneal, all hydrogen is present as either  $H_{2A}$  or BH, and that all initially present  $H_{2A}$  dimers form BH pairs and dissociate again according to Equation (1) during dark annealing, the fit parameter  $A_2$  from Equation (2) can be used as a measure for the total amount of hydrogen within the  $H_{2A} \rightleftharpoons BH$  subsystem. Putting the two quantities  $\Delta[BH]_{t=0h}$  and  $\Delta[BH]_{DA}$  in relation to  $A_2$ , it can be seen that at high firing temperatures, the ratio  $\Delta[BH]_{t=0h}/A_2$  is about 20%, and that of  $\Delta[BH]_{DA}/A_2$  is about 80%. Interestingly, this ratio changes with lower firing temperatures. The proportion of  $\Delta[BH]_{t=0h}$  rises to almost 40%, whereas  $\Delta[BH]_{DA}$  decreases accordingly. It is difficult to imagine that the peak firing temperature itself is the underlying reason, because BH pairs become unstable at these high temperatures and tend to dissociate as will be shown in the following experiments. Furthermore, the cool-down ramp, during which the BH pairs might form again, is quite comparable for the different peak temperatures.

#### 4.2. Bare Samples

An important question to ask is whether the incorporation of hydrogen from the  $SiN_x:H$  layer really is the only source of hydrogen, which is found inside the wafer later on. Taking the idea of the origin of hydrogen far back in the history of sample fabrication, the question arises whether Si wafers are free of hydrogen in the as-delivered state from the manufacturer. The FZ-Si wafers used in this section did not receive any processing steps before electrical contacting apart from a firing step while one wafer was left unfired as a reference. This reference wafer (black stars in **Figure 3**) shows a slight increase in BH pair concentration after an initial drop. After  $\approx 2$  h of dark annealing at

220°C, the dissociation reaction of the BH pairs predominates, and  $\Delta[BH]$  declines again. Thus, it can be followed that there is already an initial hydrogen concentration of nearly  $3 \times 10^{14} \text{ cm}^{-3}$  in the purchased FZ-Si wafer, primarily in the form of BH pairs. It is unclear, whether the initial drop from the first to the second measurement point is related to BH pairs or not. It is a reproducible feature, which will be discussed in more detail in the next section. As it is not describable by the three-state system introduced earlier, the first measurement value is ignored for the fitting procedure for the time being. The amount of hydrogen in this sample seems surprisingly high, as it is even more than a wafer contains, which was passivated with hydrogen-rich  $SiN_x:H$  and fired at about 740°C (see **Figure 2**). As the same starting material was used, it is conceivable that initially present hydrogen effuses during  $SiN_x:H$  deposition at a temperature of 400°C.<sup>[22,23]</sup> Alternatively, if conversion to an energetically more favorable binding state (e.g.,  $H_{2C}$ ) or bonding to other impurities occurs, this hydrogen fraction would have escaped observation by the methodology used here.

If such a bare wafer is fired in a belt furnace, the initial concentration of BH pairs is reduced significantly (red, orange, and yellow squares in **Figure 3**). During the subsequent dark anneal, BH pairs form again. The maximum amplitude of BH pairs is  $2.8 \times 10^{14} \text{ cm}^{-3}$  for both the unfired sample and the sample fired at 533°C. This suggests that no hydrogen is lost from the  $H_{2A} \rightleftharpoons BH$  system. As the firing temperature increases, both the initial concentration of BH pairs and the maximum amplitude decrease. The former suggests that with higher peak temperature, less BH pairs form again during the cool down, or more BH pairs were dissociated in the first place. The latter implies that increasingly more hydrogen is lost from the  $H_{2A} \rightleftharpoons BH$  system—either by effusion, conversion to  $H_{2C}$  or bonding to other impurities.

To have a closer look at changes in the hydrogen system, the quantities  $\Delta[BH]_{t=0h}$  and  $\Delta[BH]_{DA}$  are plotted again as a function

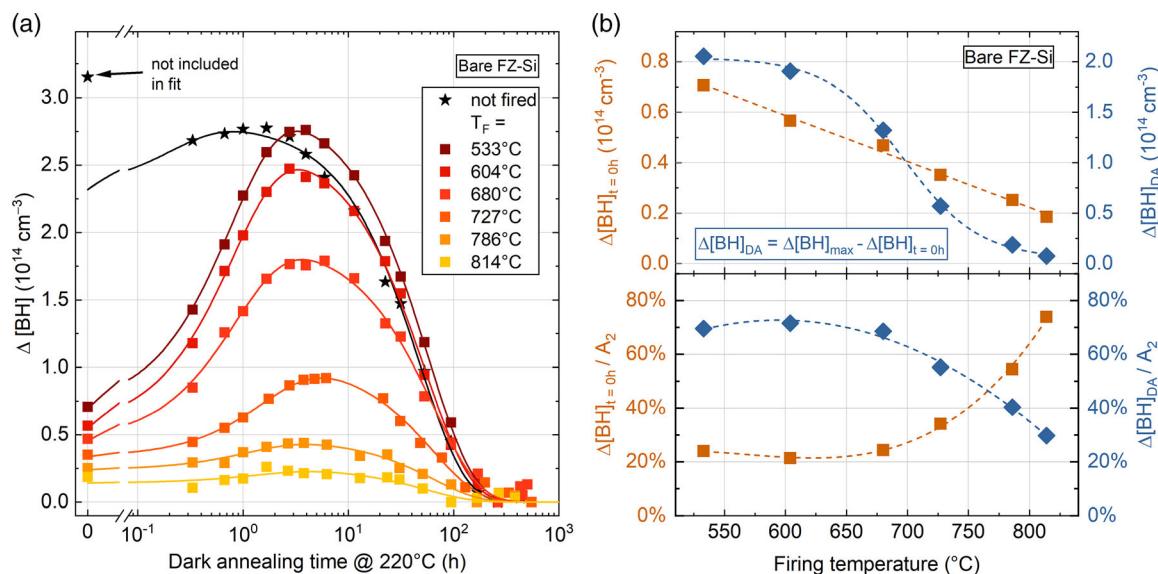


**Figure 3.** a) Change in BH pair concentration of bare, fired FZ-Si samples during a dark anneal at  $T_{DA} = 220^\circ\text{C}$ . The long-term limit is used as the reference point for calculation of  $\Delta[BH]$ . The lines are double exponential fits to the measurements according to Equation (2). b) Initial concentration  $\Delta[BH]_{t=0h}$  (brown) and increase of BH pairs during dark annealing  $\Delta[BH]_{DA}$  (blue) as a function of firing temperature. The upper graph shows absolute values, whereas the lower displays the ratio of the two quantities to the fit parameter  $A_2$ . The lines are empirical trend lines.

of firing temperature in Figure 3b. The initial BH pair concentration decreases linearly with increasing firing temperature, whereas  $\Delta[\text{BH}]_{\text{DA}}$  shows a sigmoidal decrease with strongest reduction in the range around 700 °C. The ratios with respect to  $A_2$  illustrate that a firing step around 600 °C can maximize the ratio  $H_{2A}/\text{BH}$  in the initial state. However, in doing so, the total amount of hydrogen in the system  $H_{2A} \rightleftharpoons \text{BH}$  is already decreasing. At the highest firing temperature (814 °C), a total of only  $0.2 \times 10^{14} \text{ cm}^{-3}$  hydrogen remains and is almost completely paired to boron after firing.

The change of the ratios with firing temperature is exactly opposite to that of samples with a  $\text{SiN}_x:\text{H}$  layer. This can be explained by the inverse dependence of the total hydrogen content on the firing temperature of the two sample systems with and without a  $\text{SiN}_x:\text{H}$  layer, respectively. In Figure 4, the initial fraction of BH pairs from Figure 2 and 3 relative to the hydrogen content within the  $H_{2A} \rightleftharpoons \text{BH}$  system is plotted. Calculations from Voronkov and Falster<sup>[16]</sup> (black line) show a good agreement apart from some scattering, although they used a slightly different doping ( $1 \times 10^{16} \text{ cm}^{-3}$  instead of  $1.5 \times 10^{16} \text{ cm}^{-3}$ ).

All these observations can be explained coherently if the as-purchased wafers already contain a concentration of about  $3 \times 10^{14} \text{ cm}^{-3}$  hydrogen, with around 80% present as BH pairs and 20% as  $H_{2A}$ . Subsequent processing steps at elevated temperature change this configuration. Samples with a  $\text{SiN}_x:\text{H}$  layer and fired at  $T_F = 730$  °C interestingly show a lower hydrogen concentration within the  $H_{2A} \rightleftharpoons \text{BH}$  system compared with bare samples fired at around  $T_F = 500 - 600$  °C. One possible explanation could be the following: For passivated samples, the hydrogen initially present in the as-purchased wafer is, at some point prior to dark annealing brought into a configuration in which it no longer forms BH

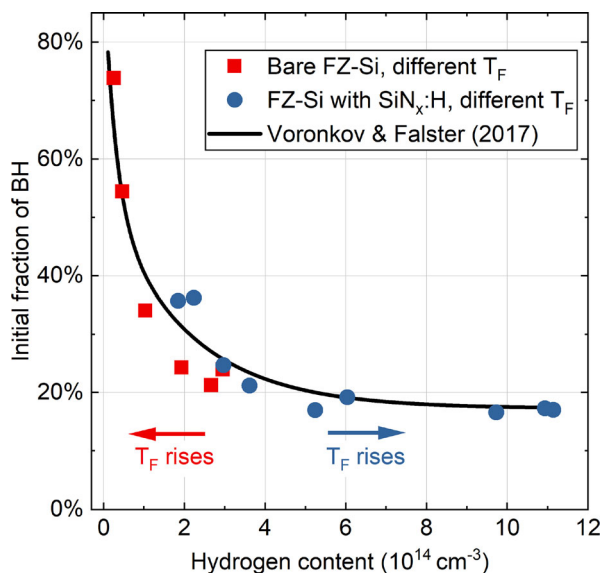


**Figure 4.** Initial fraction of BH pairs  $\Delta[\text{BH}]_{t=0h}/A_2$  after the firing step as a function of the total hydrogen content inside the  $H_{2A} \rightleftharpoons \text{BH}$  subsystem, which can be identified with the fit parameter  $A_2$ . The solid black line represents calculations made by Voronkov and Falster<sup>[16]</sup> under the following conditions:  $N_{\text{dop}} = 1 \times 10^{16} \text{ cm}^{-3}$ , firing step with a peak temperature of 750 °C and  $100 \text{ K s}^{-1}$  cooling rate. The cooling ramp is comparable to the firing profile used here.

pairs during subsequent dark annealing and is, therefore, not observable with the methodology used in this article. Hydrogen effusion out of the wafer would be an alternative explanation for the observations. It can be expected that even lower firing temperatures would reduce the amount of hydrogen in the passivated samples even more. This would imply that some hydrogen is already lost from the  $H_{2A} \rightleftharpoons \text{BH}$  system during the  $\text{SiN}_x:\text{H}$  deposition.

The question now is where does this hydrogen in the as-purchased wafer originates from in the first place. In some cases, studies assume that wafers are free of hydrogen prior to explicit contact with hydrogen-containing atmospheres or hydrogen-rich layers.<sup>[24]</sup> In fact, no formation of BH pairs is found in studies with unfired  $\text{SiN}_x:\text{H}$  layers.<sup>[13]</sup> However, the statement that a wafer is “hydrogen-free” must be treated with great caution (see the analysis in the study given by Hallam et al.<sup>[25]</sup>). There are reports in the literature that hydrogen incorporation into silicon is possible by wet chemical etching and cleaning steps.<sup>[26–28]</sup> In a surface-near region, a rather high fraction of dopant atoms will then be deactivated. It should be noted again that the used methodology only gives an integral value of  $\Delta[\text{BH}]$  with respect to the wafer volume; thus, surface effects cannot be investigated. Though, after a firing step, it can be assumed that hydrogen concentration is rather uniform throughout the wafer.<sup>[29]</sup> The presented results show that great care should be taken when investigating the role of hydrogen, because hydrogen can already be present in the wafer or introduced unintentionally, e.g., by standard wet-chemical processing steps.

### 4.3. Temperature-Dependent BH Dynamics

As shown earlier, a firing step with temperatures around 530 °C dissolves existing BH pairs, whereas a treatment at 220 °C initiates their formation. To gain more insight into the reaction dynamics, the dark annealing temperature has been varied between 200 and 290 °C on bare samples. The results for samples treated with a high-temperature firing step with hydrogen predominantly existing as  $H_{2A}$  in the beginning are shown in Figure 5a. With increasing dark annealing temperatures, the amplitude of BH pairs lowers, and the formation occurs earlier. For temperatures above 240 °C, a sharp increase occurs for prolonged annealing after dissociation of BH pairs, which is probably not related to the BH dynamics described previously. The step rise of this still unknown effect shifts to lower time constants with increasing temperature, indicating that it is thermally activated. The trend of BH associated peaks getting shallower with higher temperatures reverses at 290 °C. We, therefore, conclude that some change in BH dynamics occurs at this temperature, which causes the deviation from the trends found at lower temperatures.

In the case of unfired samples with hydrogen mainly existing as BH in the beginning, the resulting measurements are displayed in Figure 5b. The behavior at the very beginning of the treatment is dominated by a fast drop in resistance, which is interpreted as a change in BH pair density based on the measurement analysis procedure. Whether this is actually the case and which physical cause is responsible for this cannot be answered on the basis of these data. Diffusion dynamics might play a role here, because hydrogen is expected to exist mainly close to the surface in these unfired samples, but a separate system completely

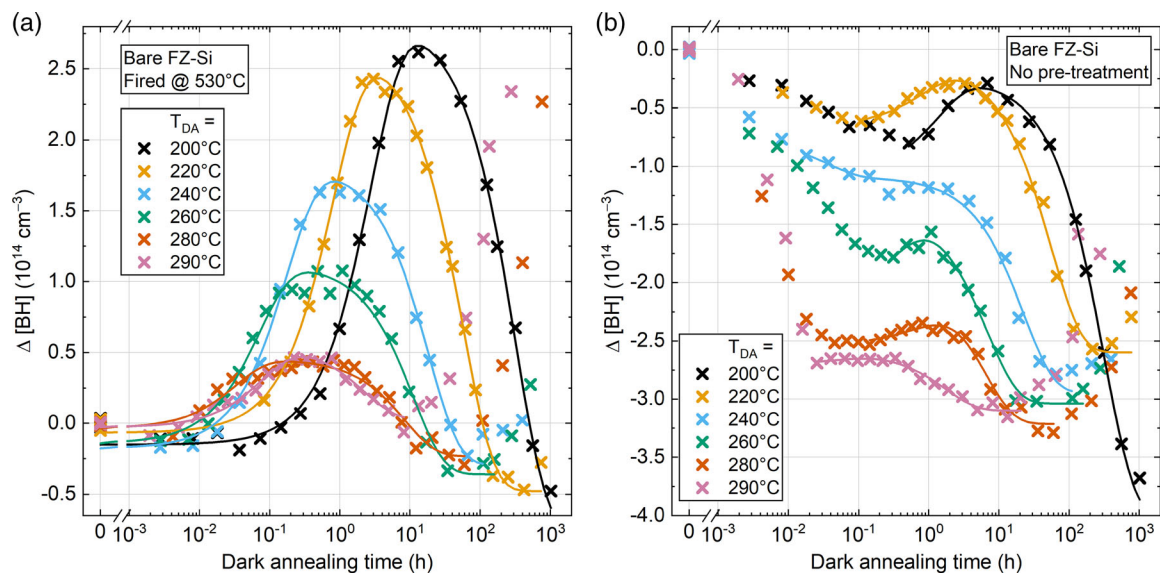


**Figure 5.** a) Calculated change in BH concentration for fired samples under a dark annealing procedure. A higher dark annealing temperature leads to lower amplitudes and an accelerated dynamics. Change in BH concentration is calculated with respect to the initial resistance measurement. b) Calculated change in BH concentration for bare, unfired samples. The amplitude of the local maximum decreases with increasing temperature. Change in BH concentration is calculated with respect to the initial resistance measurement, and the lines are fits according to Equation (2).

unrelated to BH dynamics also changing hole concentration is conceivable as well. However, as the focus of this work is on the dynamics for longer times, this particular feature will not be evaluated further. This effect is followed by a local maximum that becomes flatter for rising temperatures and shifts to shorter times. As the maximum disappears for 290 °C, the validity of the model below this temperature can also be shown here.

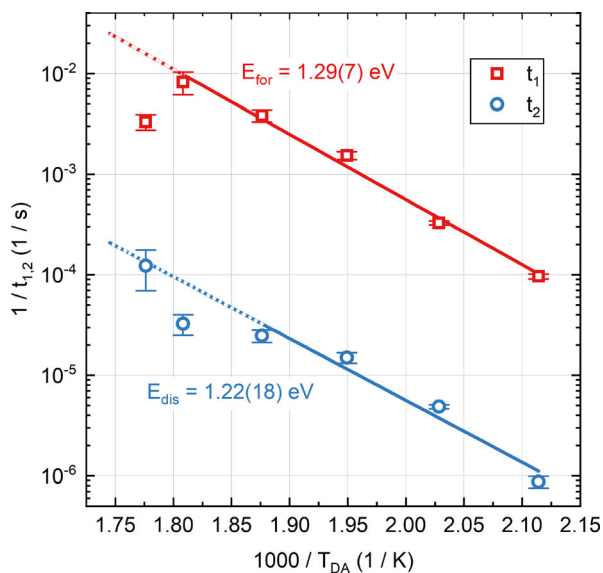


**Figure 6.** The fit parameters of the effective time constants  $t_{1,2}$  for formation and dissociation from Figure 5a are shown as an Arrhenius plot. Error bars show one standard deviation obtained from fitting. Solid lines indicate the range of values included in the linear regression. The dotted line shows how the parameters for high temperatures deviate from it.

If we examine the fitted time constants of Figure 5a more closely, we arrive at the representation in Figure 6. Shown are the inverse time constants  $t_{1,2}$  for formation and dissociation of BH pairs versus inverse temperature. Note that this is a phenomenological approach, referring only to the effective reaction rates of the system. By assuming an Arrhenius-like dependence of the time constants, the effective activation energy of the formation of BH pairs  $E_{for} = 1.29(7) \text{ eV}$  and of the dissociation  $E_{dis} = 1.22(18) \text{ eV}$  can be determined. For the regression, only values in the range of the solid line were included. Again, it can be stated here that above 280 °C, a change takes place. The selection of the values included in the Arrhenius fit for the dissociation reaction was deliberately set narrow, because for higher temperatures, the dissociation is strongly influenced by the strong long-term increase described earlier.

The time constants of the case of unfired samples (Figure 5b), on the other hand, are strongly influenced by the initial drop and, therefore, exhibit large uncertainties, which would make an analysis not very meaningful.

## 5. Conclusion

In this article, the dynamics of BH pairs in boron-doped FZ-Si during dark annealing is investigated using highly accurate resistance measurements. As-purchased, chemically polished FZ-Si wafers are found to contain a considerable amount of hydrogen, most of it paired to boron. Subsequent temperature treatment, e.g., a PECVD process or a firing process, changes the state of this hydrogen. A short high-temperature firing step applied to Si wafers coated with  $\text{SiN}_x\text{:H}$  introduces additional hydrogen into the wafer volume. After firing, it is mainly in the form of  $\text{H}_{2A}$ , but some BH pairs are also present. If a firing step with a peak temperature of around

530 °C is applied to bare, unpassivated Si wafers, most of the initially present BH pairs split up and form H<sub>2A</sub> while almost no hydrogen is lost from the H<sub>2A</sub> ⇌ BH system. With higher firing temperatures, more and more hydrogen is lost from this system. As a consequence, the share of BH pairs increases, which is in accordance with theory. Furthermore, it could be shown that with increasing dark annealing temperature, the BH dynamics accelerates, whereas the maximum BH concentration reached decreases. The three-state model used to mathematically describe BH dynamics shows very good agreement with measurement data for both bare and passivated silicon, as well as for different annealing temperatures. Effective activation energies for formation and dissociation of BH pairs are determined to be 1.29(7) and 1.22(18) eV, respectively. For temperatures above 280 °C, significant changes in the reaction dynamics occur, which manifests itself in a deviation of the time constants from Arrhenius behavior. Besides BH pair formation and dissociation, which is well described in the model used, two additional thermally activated effects were found to have an impact on hole concentration. The first one happens rather fast and is occurring predominantly in unfired wafers only. The second occurs for prolonged annealing times and overlaps with the dissociation reaction for temperatures above 240 °C.

## Acknowledgements

The authors want to thank Barbara Rettenmaier for technical support. Part of this work was supported by the German Federal Ministry of Economic Affairs and Energy under contract number 03EE0152A. The content is the responsibility of the authors.

Open access funding enabled and organized by Projekt DEAL.

## Conflict of Interest

The authors declare no conflict of interest.

## Data Availability Statement

Research data are not shared.

## Keywords

boron–hydrogen pairs, dark annealing, firing, float-zone silicon, hydrogen

Received: April 15, 2021

Revised: June 2, 2021

Published online: July 8, 2021

- [1] J. I. Pankove, D. E. Carlson, J. E. Berkeyheiser, R. O. Wance, *Phys. Rev. Lett.* **1983**, *51*, 2224.
- [2] S. J. Pearton, J. W. Corbett, T. S. Shi, *Appl. Phys. A* **1987**, *43*, 153.
- [3] A. G. Aberle, *Progr. Photovolt. Res. Appl.* **2000**, *8*, 473.
- [4] C. Herring, N. M. Johnson, C. G. Van de Walle, *Phys. Rev. B* **2001**, *64*, 125209.
- [5] C. G. Van De Walle, P. J. Denteneer, Y. Bar-Yam, S. T. Pantelides, *Phys. Rev. B* **1989**, *39*, 10791.
- [6] S. Wilking, S. Ebert, A. Herguth, G. Hahn, *J. Appl. Phys.* **2013**, *114*, 194512.
- [7] M. A. Jensen, A. Zuschlag, S. Wiegold, D. Skorka, A. E. Morishige, G. Hahn, T. Buonassisi, *J. Appl. Phys.* **2018**, *124*, 085701.
- [8] T. H. Fung, M. Kim, D. Chen, C. E. Chan, B. J. Hallam, R. Chen, D. N. Payne, A. Ciesla, S. R. Wenham, M. D. Abbott, *Sol. Energy Mater. Sol. Cells* **2018**, *184*, 48.
- [9] D. Chen, P. Hamer, M. Kim, C. Chan, A. Ciesla nee Wenham, F. Rougieux, Y. Zhang, M. Abbott, B. Hallam, *Sol. Energy Mater. Sol. Cells* **2020**, *207*, 110353.
- [10] J. Schmidt, D. Bredemeier, D. C. Walter, *IEEE J. Photovolt.* **2019**, *9*, 1497.
- [11] C. Sah, J. Y. Sun, J. J. Tzou, *Appl. Phys. Lett.* **1983**, *43*, 204.
- [12] A. J. Tavendale, D. Alexiev, A. A. Williams, *Appl. Phys. Lett.* **1985**, *47*, 316.
- [13] D. C. Walter, D. Bredemeier, R. Falster, V. V. Voronkov, J. Schmidt, *Sol. Energy Mater. Sol. Cells* **2019**, *200*, 109970.
- [14] A. Herguth, C. Winter, *IEEE J. Photovolt.* **2021**, *11*, 1059.
- [15] R. E. Pritchard, J. H. Tucker, R. C. Newman, E. C. Lightowers, *Semicond. Sci. Technol.* **1999**, *14*, 77.
- [16] V. V. Voronkov, R. Falster, *Phys. Status Solidi B* **2017**, *254*, 1600779.
- [17] R. S. Bonilla, B. Hoex, P. Hamer, P. R. Wilshaw, *Phys. Status Solidi A* **2017**, *214*, 1700293.
- [18] M. J. Binns, S. A. McQuaid, R. C. Newman, E. C. Lightowers, *Semicond. Sci. Technol.* **1993**, *8*, 1908.
- [19] E. Schneiderlöchner, R. Preu, R. Lüdemann, S. W. Glunz, *Progr. Photovolt. Res. Appl.* **2002**, *10*, 29.
- [20] PV Lighthouse, Mobility Calculator, <https://www2.pvlighthouse.com.au/calculators/mobility%20calculator/mobility%20calculator.aspx> (accessed: April 2021).
- [21] D. Bredemeier, D. C. Walter, R. Heller, J. Schmidt, *Phys. Status Solidi* **2019**, *13*, 1900201.
- [22] M. Stutzmann, W. Beyer, L. Tapfer, C. P. Herrero, *Phys. B: Condens. Matter* **1991**, *170*, 240.
- [23] W. Beyer, *Phys. B: Condens. Matter* **1991**, *170*, 105.
- [24] D. C. Walter, J. Schmidt, *Sol. Energy Mater. Sol. Cells* **2016**, *158*, 91.
- [25] B. J. Hallam, P. G. Hamer, A. M. Ciesla née Wenham, C. E. Chan, B. V. Stefani, S. Wenham, *Progr. Photovolt. Res. Appl.* **2020**, *28*, 1217.
- [26] A. J. Tavendale, A. A. Williams, S. J. Pearton, *MRS Proc.* **1987**, *104*, 285.
- [27] B. Sopori, Y. Zhang, N. M. Ravindra, *J. Electron. Mater.* **2001**, *30*, 1616.
- [28] J. Weber, S. Knack, O. Feklisova, N. Yarykin, E. Yakimov, *Microelectron. Eng.* **2003**, *66*, 320.
- [29] M. Sheoran, D. S. Kim, A. Rohatgi, H. F. Dekkers, G. Beaucarne, M. Young, S. Asher, *Appl. Phys. Lett.* **2008**, *92*, 172107.